

Tuning the Interfacial Properties of Grafted Chains with a pH Switch

X. Zhu,[†] J. DeGraaf,[‡] F. M. Winnik,^{‡,§} and D. Leckband^{*,†,⊥}

Department of Chemical and Biomolecular Engineering, University of Illinois at Urbana-Champaign, 600 South Mathews Avenue, Urbana, Illinois 61801, Department of Chemistry and Faculty of Pharmacy, University of Montreal, Montreal, Quebec, Canada, Department of Chemistry, University of Illinois at Urbana-Champaign, 600 South Mathews Avenue, Urbana, Illinois 61801, and Department of Chemistry, McMaster University, Hamilton, Ontario, Canada

Received August 6, 2003. In Final Form: October 29, 2003

Environmentally responsive, water-soluble polymers have a wide variety of uses ranging from drug delivery to viscosity modifiers. Their utility lies in the ability to use environmental perturbations to dramatically alter the material properties. Here, we describe the interfacial properties of a hydrophobically modified copolymer of *N*-isopropylacrylamide and glycylacrylamide (NIPAM-*N*-Gly-(C18)₂), which is both temperature and pH responsive. Direct force measurements quantified the substantial pH-dependent change in the molecular properties of end-grafted NIPAM-*N*-Gly-(C18)₂ monolayers. At pH 8.0, where the glycine side chains are ionized, the polymers exhibit stereotypical polyelectrolyte behavior. Side chain neutralization at pH 5.0 causes a substantial decrease in the film thickness, and the polymer films adhere strongly. The adhesion is presumably through H-bonding between the glycine side chains. Our findings revealed the likely molecular basis of pH-dependent changes in the copolymer films and identified clear design criteria for tuning the interfacial properties of these polymer films.

Introduction

Surface-grafted polymers are widely used to imbue materials surfaces with desired properties for specific engineering applications. The advantages of this methodology are linked to the wide variety of polymers and a corresponding range of interfacial properties. Most surface modification strategies rely on tailoring the material's surface properties with a single surface chemistry, but the surface properties, and hence the material interactions, of environmentally responsive "smart" polymers can be reversibly switched on demand.^{1,2} Such polymers undergo environmentally triggered phase transitions in response to distinct environmental stimuli. One such temperature responsive material is poly(*N*-isopropylacrylamide) (PNIPAM).

Most studies of PNIPAM have focused on its temperature-dependent phase behavior.^{3–6} PNIPAM undergoes a temperature-triggered, reversible change in aqueous solubility at the lower critical solution temperature (LCST) of 32 °C. That the latter is conveniently close to body temperature makes PNIPAM a potentially useful material for thermally controlled drug delivery in vivo.³ PNIPAM is hypothesized to swell in water below the transition

temperature, adopting a random coil configuration. Above the LCST, the chains are believed to become more hydrophobic and to collapse into a globular conformation.^{7,8} This thermoresponsive property has been used to fabricate functional hydrogels,⁹ tissue glues,¹⁰ and membranes.^{11,12} Atomic force microscopy investigations reported significant temperature-induced changes in the range of repulsion by PNIPAM films.⁴ Yakushiji and co-workers found that graft architecture affects the wettability changes of PNIPAM-modified surfaces.⁵

In addition to temperature, several pH-responsive polymers collapse or expand in response to pH shifts. Some of these materials were developed to overcome some practical limitations of liposome delivery systems. Following cell internalization, liposomes are trafficked to lysosomes where their contents may be degraded by various hydrolases and peptidases. This often leads to the poor cytoplasmic transfer of labile compounds, which may not easily cross cell membranes.⁶ A potential solution is to design liposomes that only release their contents when exposed to mild acidic conditions. The polymer structure would be such that, in acidic environments, configurational changes in the adsorbed polymers would promote liposome disruption.^{13–15} Examples of pH-responsive polymers that have shown promising

* To whom correspondence may be addressed: telephone, 217-244-0793; fax, 217-333-5052; e-mail, leckband@scs.uiuc.edu.

[†] Department of Chemical and Biomolecular Engineering, University of Illinois at Urbana-Champaign.

[‡] Department of Chemistry, McMaster University.

[§] Department of Chemistry and Faculty of Pharmacy, University of Montreal.

[⊥] Department of Chemistry, University of Illinois at Urbana-Champaign.

(1) Galaev, I. Y. *Adv. Colloid Interface Sci.* **1999**, *17*, 335–340.

(2) Hoffman, A. *Artif. Organs* **1995**, *19*, 458–467.

(3) Schild, H. G. *Prog. Polym. Sci.* **1992**, *17*, 163–249.

(4) Kidoaki, S.; Ohya, S.; Nakayama, Y.; Matsuda, T. *Langmuir* **2001**, *17*, 2402–2407.

(5) Yakushiji, T.; Sakai, K.; Kikuchi, A.; Aoyagi, T.; Sakurai, Y.; Okano, T. *Anal. Chem.* **1999**, *71*, 1125–1130.

(6) Huang, A.; Kennel, S.; Huang, L. *J. Biol. Chem.* **1983**, *258*, 14034–14040.

(7) Heskins, M.; Guillet, J. E. *J. Macromol. Sci. Chem.* **1968**, *A2*, 1441–1455.

(8) Wang, X.; Qiu, X.; Wu, C. *Macromolecules* **1998**, *31*, 2972–2976.

(9) Dong, L. C.; Hoffman, A. S. *ACS Symp. Ser.* **1987**, *No. 350*, 216–244.

(10) Matsuda, T.; Moghaddam, M. J. *Mater. Sci. Eng.* **1993**, *C1*, 37–43.

(11) Iwata, H.; Oodate, M.; Uyama, Y.; Amemiya, H.; Ikada, Y. *J. Membr. Sci.* **1991**, *55*, 119–130.

(12) Yamada, K.; Sato, T.; Tatekawa, S.; Hirata, M. *Polym. Gels Networks* **1994**, *2*, 323–331.

(13) Meyer, O.; Papahadjopoulos, D.; Leroux, J. C. *FEBS Lett.* **1998**, *421*, 61–64.

(14) Chen, T.; Choi, L. S.; Einstein, S.; Klippenstein, M. A.; Scherrer, P.; Cullis, P. R. *Liposome Res.* **1999**, *9*, 387–405.

(15) Franzin, C. M.; MacDonald, P. M.; Polozova, A.; Winnik, F. M. *Biochim. Biophys. Acta* **1998**, *1415*, 219–234.

liposome release characteristics, include poly(alkyl acrylic acid)^{14,16,17} and copolymers of PNIPAM.¹⁸

Exploiting the observations of Schneider and co-workers,¹⁹ it was shown that the introduction of amino acid side chains into copolymers backbones could also imbue polymers with pH sensitivity. Force measurements with glycine-functionalized amphiphiles showed that glycine side chains not only alter the electrostatic properties of membrane surfaces but also promote adhesion over certain pH ranges.¹⁹ Principi and co-workers²⁰ showed that the LCST of copolymers of *N*-isopropylacrylamide and *N*-glycidylacrylamide depended strongly on pH. Subsequent studies investigated the stability and pH sensitivity of vesicles coated with the hydrophobically modified copolymer both in buffer and in human serum. At pH 7.2, vesicles coated with this material were stable for over 90 days at 4 °C. Above the LCST of 37 °C, the polymer destabilized the vesicles under weakly acidic conditions, but in human serum at neutral pH, the polymer was only slightly destabilizing.²¹

In this work, we provide direct evidence for the molecular level changes of grafted NIPAM-*N*-glycine copolymer films that are triggered by pH changes. Using direct force measurements, we quantified the range and magnitude of both repulsive and attractive forces between the copolymer films as a function of pH. The film properties were further investigated as a function of polymer grafting density and ionic strength. These results both elucidate the molecular basis for experimentally observed changes in the interfacial properties of the coatings and define molecular design rules for tailoring the properties of end-grafted NIPAM-*N*-Gly-(C18)₂ monolayers.

Materials and Methods

Materials. High-purity 1,2-dipalmitoyl-*sn*-glycero-3-phosphoethanolamine (DPPE) and 1,2-distearoyl-*sn*-glycero-3-phosphoethanolamine (DSPE) were purchased in powder form (purity >99%) from Avanti Polar Lipids Inc. (Alabaster, AL). *N*-Isopropylacrylamide (NIPAM) was obtained from Aldrich Chemicals Co and purified by recrystallization from hexane/toluene (1/1 v/v). *N*-Acryloylglycine ethyl ester (NAGEE)²⁰ and the lipophilic initiator 4,4'-azobis(4-cyano-*N,N*-di-*n*-octadecyl)pentanamide (DODA) were prepared as previously described.²² All inorganic salts were high purity (>99.5%) and were purchased from Aldrich (Milwaukee, WI). All aqueous solutions were prepared with water purified with a Milli-Q UV-Plus water purification system (Millipore, Bedford, MA). Water had a resistivity of 18.2 MΩ cm⁻¹. HPLC grade methanol and chloroform purchased from Mallinckrodt (St. Louis, MO) were used to prepare lipid solutions. High-purity silver shot (99.99%, Aldrich) used for the preparation of silver films on the mica was from Alfa Aesar (Ward Hill, MA).

Preparation of NIPAM-*N*-Gly-(C18)₂. The copolymer was prepared in two steps, involving, first, the preparation of a copolymer of NIPAM and NAGEE and, second, the hydrolysis of the ethyl ester groups of the glycine side chains. Step 1: A solution of NIPAM (0.490 g, 4.33 mmol), NAGEE (0.684 g, 4.35 mmol), and DODA (0.153 g, 0.119 mmol) in methanol/dioxane (25 mL, 2:1 v/v) was purged with nitrogen for 1 h at room temperature. It was brought to 65 °C and stirred for 20 h under

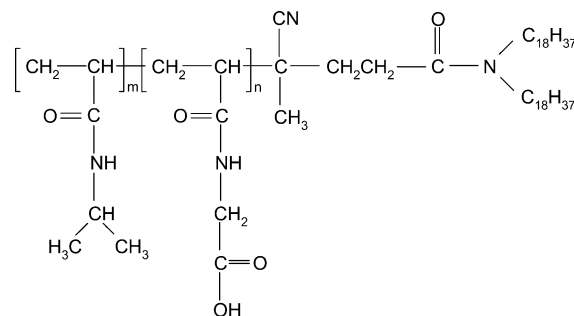


Figure 1. The structure of the NIPAM-*N*-Gly-(C18)₂ copolymer. In this study, values for *m* and *n* were 133 and 84, respectively, giving an *m/n* ratio of 1.6.

nitrogen. It was cooled to room temperature and concentrated in vacuo. The copolymer was isolated by precipitation into diethyl ether and purified by two precipitations from tetrahydrofuran (THF) into diethyl ether, yielding NIPAM-*N*-Gly-(C18)₂, ethyl ester form. This copolymer (0.500 g) was dissolved in THF/water (40 mL, 4:1 v/v) and treated with a solution of NaOH (0.08 g, 2.0 mmol) in THF/water (10 mL, 4:1 v/v). The reaction mixture was allowed to stir for 10 h. It was then brought to neutral pH by dropwise addition of aqueous HCl (1.0 M). The solution was concentrated in vacuo. The residual oil was dissolved in a minimum amount of methanol. The copolymer was isolated by precipitation into diethyl ether and purified by two additional precipitations from methanol into diethyl ether (0.478 g). The *N*-glycine-acrylamide content (NIPAM to *N*-glycine acrylamide ratio, *m/n* = 1.58 (Figure 1) was obtained by titration of the carboxylic acid groups performed with a Tanager Scientific Systems 8901 dual pH meter and titrimer coupled to a microcomputer. The average number of acrylamide units per *n*-octadecyl end groups was determined from an analysis of the ¹H NMR spectrum in CDCl₃ (Bruker AMX500 spectrometer) of the ethyl ester protected copolymer (step 1). It was calculated using the areas of the signals at 3.97 ppm, due to the resonance of the isopropylidene proton of the NIPAM units and at 4.18 ppm, attributed to the methylene protons of the glycine unit (-NH-CH₂-COO-C₂H₅), together with the area of the signal at 0.85 ppm, attributed to the resonance of the protons of the terminal methyl group of the *n*-octadecyl chains. This analysis led to a *M_n* value of 30 000 (±500). The molecular weight of the polymer was determined also by gel permeation chromatography (GPC) analysis, using polystyrene standards (*M_w* 26 000; *M_w*/*M_n* 1.7). GPC was performed with a Waters system equipped with a Waters 510 HPLC pump, a Waters 486 UV detector, and Waters 410 differential refractometer and two TSK-gel (α-M and α-3000, Tosoh Biosep, Japan) columns eluted with dimethyl formamide (0.5 mL min⁻¹ flow rate, 40 °C). Data were analyzed using the Millennium (Waters) software.

Cloud points were determined by spectrophotometric detection of the change in turbidity (λ = 600 nm) of aqueous copolymer solutions (1.0 g L⁻¹) heated at a constant rate (0.5 °C min⁻¹) in a magnetically stirred UV cell placed in a Hewlett-Packard 8452A photodiode array spectrometer equipped with a 89090A temperature controller. The LCST was >60 °C for solutions at pH >2.0. Solutions of lower pH exhibit cloud points at 33.1 °C (pH 1.23) and 38.4 °C (pH 1.86). The value reported is the temperature corresponding to a decrease of 20% of the solution transmittance.

End-Grafted NIPAM-*N*-Gly-(C18)₂ Monolayers. Solutions of NIPAM-*N*-Gly copolymer and pure DSPE were prepared in 9:1 chloroform/methanol solutions. Mixtures of various molar ratios of NIPAM-*N*-Gly-(C18)₂ with DSPE were prepared by mixing solutions of pure DSPE and lipopolymer in the appropriate proportions. Surface pressure versus area isotherms were carried out with a commercial Langmuir-Blodgett trough (NIMA Technologies, type 611), equipped with a standard Wilhelmy microbalance. In preparation of samples for experiments at pH 8, the subphase contained 10 mM HEPES and 0.01 M NaNO₃ at pH 8. For measurements at pH 5, the subphase consisted of pure water (pH ~5). The subphase was maintained at 25 °C by a circulating water jacket.

(16) Fujiwara, M.; Baldeschwieler, J. D.; Grubbs, R. H. *Biochim. Biophys. Acta* **1996**, *1278*, 59–67.

(17) Seki, K.; Tirrell, D. A. *Macromolecules* **1984**, *17*, 1692–1698.

(18) Roux, E.; Francis, M.; Winnik, F. M.; Leroux, J. F. *Int. J. Pharm.* **2002**, *242*, 25–36.

(19) Schneider, J.; Berndt, P.; Haverstick, K.; Kumar, S.; Chiruvolu, S.; Tirrell, M. *J. Am. Chem. Soc.* **1998**, *120*, 3508–3509.

(20) Principi, T.; Goh, C. C. E.; Liu, R. C. W.; Winnik, F. M. *Macromolecules* **2000**, *33*, 2958–2966.

(21) Francis, M. F.; Dhara, D.; Winnik, F. M.; Leroux, J.-C. *Bio-macromolecules* **2001**, *2*, 741–749.

(22) Kitano, H.; Akatsuka, Y.; Ise, N. *Macromolecules* **1991**, *24*, 42–46.

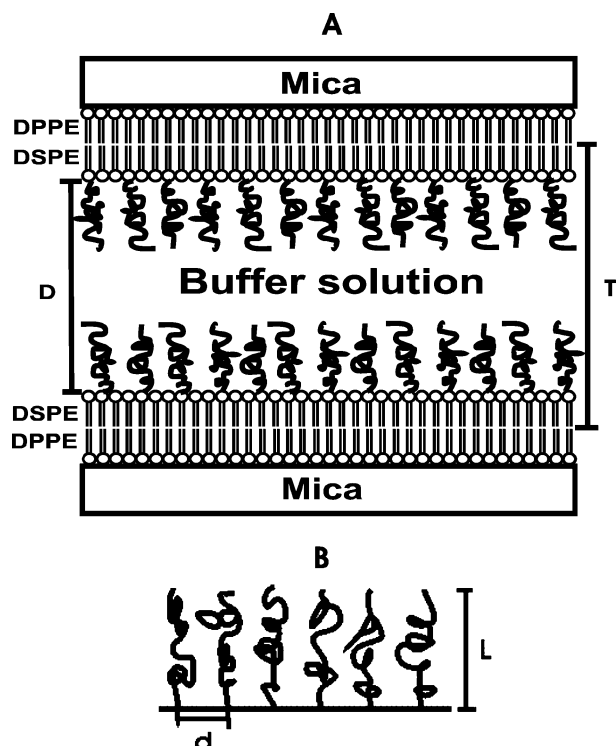


Figure 2. (A) Sample configuration used in the direct force measurements. The distances, D , reported in the text refer to the separation between the bare DSPE lipid membranes beneath the grafted NIPAM-N-Gly-(C₁₈)₂, as shown here. (B) The configuration of grafted NIPAM-N-Gly-(C₁₈)₂ chains. At the three different grafting densities used in the study (2150 ± 35 , 1048 ± 16 , 387 ± 6 Å²/chain), the polymers were in the “brush” regime. L is polymer brush extension, and d is the distance between grafting sites.

Table 1. End-Grafted NIPAM-N-Gly-(C₁₈)₁₂ Monolayers

mol % NIPAM-N-Gly-(C ₁₈) ₁₂	grafting density (Å ² /chain)	$d/2R_F$
2	2150 ± 35	0.68
4	1048 ± 16	0.47
10	387 ± 6	0.16

The bilayer was prepared by depositing a DSPE/lipopolymer monolayer onto a crystalline monolayer of DPPE (43 Å²/lipid) that was prepared by Langmuir–Blodgett (LB) deposition from the water–vapor interface onto freshly cleaved mica substrates. After the DSPE/NIPAM-N-Gly-(C₁₈)₂ mixture was spread on the water surface of the trough, it was compressed to an average area of ~ 43 Å² per lipid. The monolayer was then deposited at a constant pressure of 37 mN/m onto the supported DPPE monolayer. The transfer ratio, which is the area transferred relative to the area coated by the film, was close to unity in all cases. Adjusting the NIPAM-N-Gly-(C₁₈)₂ mole percent in the monolayer thereby enabled us to control the polymer grafting density. In this study, we used 2, 4, and 10 mol % NIPAM-N-Gly-(C₁₈)₂, corresponding to 2150 ± 35 , 1048 ± 16 , and 387 ± 6 Å²/chain, respectively (Table 1). For all three cases, the grafted polymer layers were in the brush regime (Figure 2B). The chains form brushes when the distance between polymer chains, d , is much less than twice the Flory radius, R_F .²³ The estimated Flory radius, R_F , of the glycine–NIPAM copolymer used in this work is 38 Å. The distance between polymer chains, d , is 52, 36, and 22 Å at 2, 4, and 10 mol % NIPAM-N-Gly-(C₁₈)₂ in the layer. The ratios of $d/2R_F$ are given in Table 1.

Characterization by Force Measurements. The surface force apparatus (SFA) quantifies the force between thin films confined between two crossed cylindrical surfaces as a function

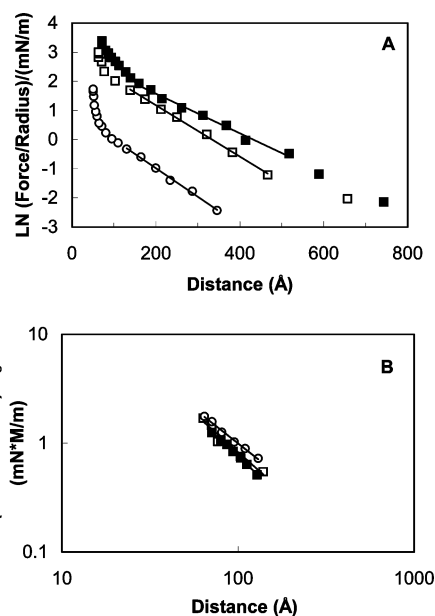


Figure 3. Normalized force vs distance between identical NIPAM-N-Gly-(C₁₈)₂ brushes at pH 8.0 at different salt concentrations. (A) Force/radius (F/R) vs distance between 4 mol % copolymer brushes at different ionic strengths. The filled squares correspond to measurements obtained in 0.05 M NaNO₃, the open squares to 0.1 M NaNO₃, and the open circles correspond to 1 M NaNO₃. Straight lines are exponential fits to the data at large distance. (B) Logarithm of the normalized force (F/R) scaled by C_s ($\ln(F C_s/R)$) vs distance at distances < 180 Å. The straight lines through the data are fits to the power law $F/R = AD^n$.

of distance between the disks. In this study, we used a Mark III surface force apparatus (SurForce Co., Santa Barbara, CA).²⁴ Measurements were carried out at 25 °C in a temperature-controlled room. This is below the measured lower critical solution temperature of > 54 °C for this copolymer. The distances are measured with a resolution of ± 1 Å with the multiple beam interferometric technique of the instrument.^{24,25} The force, normalized by the geometric average radii of the disks $R = (R_1 R_2)^{1/2}$ is determined with a resolution of ± 0.1 mN/m from the deflection of a sensitive leaf spring that supports the lower disk.²³ The normalized force $F_c(D)/R$ is related to the corresponding interaction energy per unit area $E(D)$ between two equivalent planar surfaces by the Derjaguin approximation: $E_f = F_c/2\pi R$.²³ This relationship holds when the separation distance $D \ll R$.²³

Results

Definition of Distance between surfaces D . In force measurements between grafted polymers, $D = 0$ Å is defined as contact between the lipid headgroups underneath the polymer chains. The total difference between the distances measured before and after the deposition of DSPE and polymer layer defines the total thickness T of both outer lipid monolayers plus the polymer headgroups. The distance between surfaces D was determined by subtracting the thickness of the two DSPE monolayers from the total thickness T (Figure 2A). Thus, $D = T - 2t_{\text{DSPE}}$, where the thickness of the DSPE monolayers, t_{DSPE} , is 28 Å.²⁶

Forces between End-Grafted NIPAM-N-Gly-(C₁₈)₂ Brushes at pH 8.0. The distance dependence of the normalized force between end-grafted NIPAM-N-Gly-(C₁₈)₂ monolayers at pH 8.0 is shown in Figures 3 and 4.

(24) Israelachvili, J.; McGuiggan, P. *J. Mater. Res.* **1990**, *5*, 2223–2231.

(25) Israelachvili, J. N. *J. Colloid Interface Sci.* **1973**, *44*, 259–272.

(26) Marra, J.; Israelachvili, J. *Biochemistry* **1985**, *24*, 4608–4618.

(23) Israelachvili, J. *Intermolecular and Surface forces*, 2nd ed.; Academic Press: London, 1991.

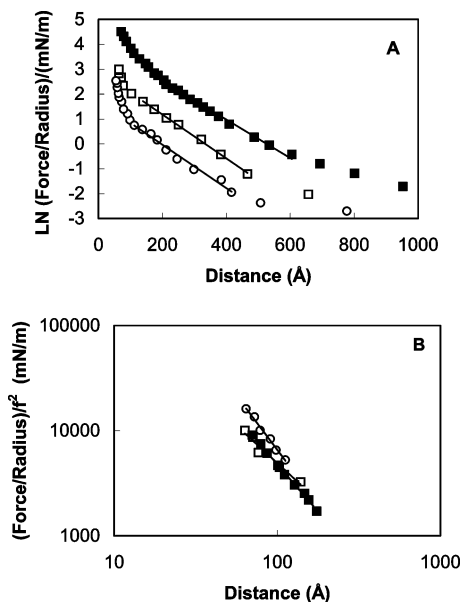


Figure 4. Normalized force vs distance between identical NIPAM-N-Gly-(C₁₈)₂ brushes at pH 8.0 as a function of grafting density. (A) Logarithm of the normalized force $\ln(F/R)$ vs distance between brushes at different polymer grafting densities. The filled squares correspond to a grafting density of 10 mol %, the open squares to 4 mol %, and the open circles to 2 mol %. The solid lines through the data show the exponential decay at large distance. (B) Normalized force, scaled by $1/f^2$ ($F/f^2/R$) vs distance, at distances <180 Å. The straight lines through the data are fits to the power law $F/R = AD^n$.

Figure 3 shows the ionic strength dependence of the forces between the brushes (4 mol %; 1048 Å²/chain), and Figure 4 shows the dependence of the force profiles on the polymer grafting density. The force profiles measured at all three ionic strengths and grafting densities were repulsive at all distances. There was no adhesion between any of these films at pH 8.

The Pincus model for polyelectrolyte brushes predicts that the force between two planar brush layers will exhibit three different dependencies on the separation distance.²⁷ At distances greater than $2L$, where L is the brush extension, the force is largely due to the double layer repulsion and should decay exponentially with the Debye length, κ^{-1} . When polyelectrolyte brushes on opposed flat plates overlap at $D < 2L$, the disjoining pressure Π exhibits two regimes. When $D > 2D^*$, where

$$D^* = N(2d^2C_s)^{-1} \quad (1)$$

the disjoining pressure scales directly with the salt concentration C_s , the distance between grafting sites d^2 , and the distance D as

$$\Pi \sim 1/(C_s d^4 D^2) \quad (2)$$

In eq 1, N is the number of monomers in the chain. When $D < D^*$, the disjoining pressure is independent of either the salt concentration or the grafting density. In our studies, D^* was always smaller than half of the distance of closest approach (repulsive “hard wall”). We therefore only analyzed forces in the regime where $D > 2D^*$.

To relate the predicted force law between two flat plates to the normalized force between the two curved disks in the SFA, we used the Derjaguin approximation.²³ Here, the potential between flat surfaces W_{f-f} is related to the

Table 2. Scaling Parameters for Force Profiles between NIPAM-N-Gly-(C₁₈)₂ Brushes at pH 8.0

grafting density (Å ² /chain)	power law exponent (decay length (Å))		
	0.05 M	0.1 M	1.0 M
2150		-2.1 ± 0.1 (115 ± 3)	
1048	-1.52 ± 0.04 (147 ± 14)	-1.4 ± 0.2 (114 ± 9)	-1.27 ± 0.05 (98 ± 3)
387		-1.80 ± 0.04 (130 ± 2)	

force between a sphere of radius R and plane (or between two crossed cylinders) by $F_{s-f} = 2\pi R W_{f-f}$. Thus, the distance dependence of F_{s-f}/R at $D^* < D < 2L$ is

$$F_{s-f}/R \sim 1/(C_s d^4 D) \quad (3)$$

Because d^2 , the grafting density, is proportional to the mole fraction of the lipopolymer in the lipid layer, f , we can rewrite eq 2 as

$$F_{s-f}/R \sim f^2/(C_s D) \quad (4)$$

Equations 2 and 3 show that the normalized force profiles measured between polyelectrolyte brushes on two crossed cylinders will scale with $1/D$, with f^2 , and with $1/C_s$.

The thickness of the polyelectrolyte brush, L , also depends on the salt concentration and on the grafting density according to

$$L \sim (C_s/f)^{-1/3} \quad (5)$$

To determine the effects of the salt concentration C_s on the force profiles, we performed the force measurements at three different NaNO₃ concentrations: namely, 0.01, 0.1, and 1 M NaNO₃ at pH 8.0. Figure 3A shows the effect of ionic strength on the normalized force curves measured between NIPAM-N-Gly-(C₁₈)₂ at 1048 Å²/chain (4 mol %). Both the range and the magnitude of the repulsive force significantly decreased with increasing ionic strength. In particular, the onset of the repulsive force was at ~ 1000 , ~ 750 , and ~ 350 Å in 0.01, 0.1, and 1 M NaNO₃, respectively. The normalized force profiles also exhibit two regimes, which each display different scaling behavior with distance. At $D > 140$ Å, the force decays exponentially with distance (Figure 3A, bold lines). With 0.01 M NaNO₃, the force decays exponentially with a decay length of 147 ± 14 Å. In a 0.1 M NaNO₃ solution, the decay length is 114 ± 9 Å, and in 1 M NaNO₃, the decay length is 98 ± 3 Å. These results are summarized in Table 2.

If the data are scaled by C_s (cf. eq 2), then the force profiles at short distance ($D < 180$ Å) collapse onto a universal curve (Figure 3B). In this regime, the forces increased more sharply (cf. Figure 3A), and scaled as a power law with distance. The logarithm of the force scales linearly with distance, D (Figure 3B). Fitting the data to a simple power law gave exponents of -1.52 ± 0.04 , -1.4 ± 0.2 , and -1.27 ± 0.05 , measured in 0.05, 0.1, and 1 M NaNO₃, respectively (Table 2).

Forces between polyelectrolyte brushes should also depend on the polymer grafting density. To determine whether this applies for the NIPAM-N-Gly-(C₁₈)₂ copolymer at pH 8.0, we measured the force curves between the copolymer brushes at the different grafting densities of 2150, 1048, and 387 Å²/chain, respectively. The results shown in Figure 4A were all obtained with pH 8.0 buffer containing 0.1 M NaNO₃. At large distance, the inter-

(27) Pincus, P. *Macromolecules* **1991**, *24*, 2912–2919.

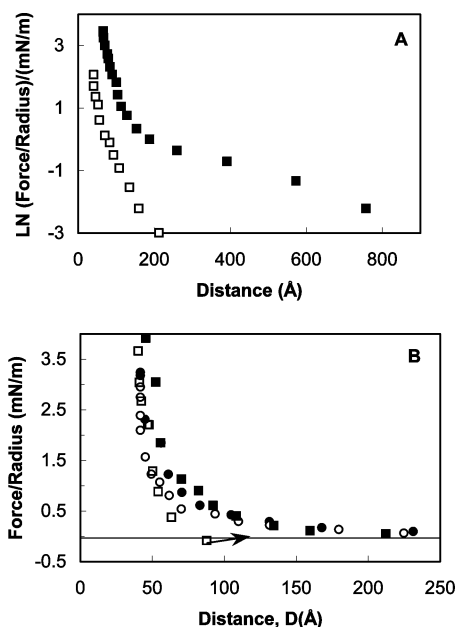


Figure 5. (A) Logarithm of the normalized force $\ln(F/R)$ versus distance between grafted NIPAM-N-Gly-(C₁₈)₂ at pH 5.0. The filled squares correspond to 10 mol % NIPAM-N-Gly-(C₁₈)₂ (387 Å²/chain) and the open squares correspond to 4 mol % NIPAM-N-Gly-(C₁₈)₂ (1048 Å²/chain). (B) Force–distance profile between 4 mol % NIPAM-N-Gly-(C₁₈)₂ monolayers at pH 5 and 25 °C. The filled squares correspond to the advancing curve in water. The open squares correspond to the receding curve in water. The filled and open circles correspond to the advancing and receding curves in an aqueous solution of 0.1 M NaNO₃ at pH 5. There was no adhesion in the latter case.

surface force decays exponentially with increasing distance (Figure 4A). At the grafting density of 2150 Å²/chain, the decay length was 115 Å at $D > 174$ Å. At 1048 Å²/polymer, the decay length was 114 Å at $D > 139$ Å and 130 Å at $D > 112$ Å between brushes at 387 Å²/chain. The decay length increased slightly at the highest grafting density.

The force–distance profiles should also scale with the inverse square of the grafting density, f^{-2} , or with d^{-4} , where d is half the distance between grafting sites. Figure 4B shows that these force profiles do exhibit the expected universal scaling behavior when the force profiles, measured with different surface grafting densities but at the same ionic strength, are scaled by f^{-2} . In the steeply increasing force region, the logarithm of the force decays linearly with distance, indicating that these data display a power law dependence on distance. The exponents, determined from fits to the data in this regime (Figure 4B) were -2.1 ± 0.1 , -1.6 ± 0.2 , and -1.80 ± 0.04 for the low, intermediate, and high grafting densities, respectively.

Forces between End-Grafted NIPAM-N-Gly-(C₁₈)₂ Brushes at pH 5.0. Decreasing the pH reduces the number of charged carboxylic acid groups ($pK_a \sim 4$) on the glycine side chains. This is expected to have three effects. First, the polyelectrolyte should become less swollen, thereby decreasing L . Second, both interchain and intrachain H-bonding may occur. Third, the reduced charge density will decrease the intersurface repulsion.

To test the impact of pH on the interfacial properties of the NIPAM-N-Gly copolymer, we carried out measurements between brushes at grafting densities of 1048 and 387 Å²/chain (Figure 5A). The initial measurements were done in 10 mM HEPES buffer without added salt. Under these conditions, the surfaces repelled at large distances, with the repulsion between the more densely grafted

Table 3. NIPAM-N-Gly-(C₁₈)₁₂ Adhesion at pH 5.0

4 mol % NIPAM-N-Gly-(C ₁₈) ₁₂ (1048 Å ² /chain)				
compressive force (mN/m)	time in contact (min)	jump-off distance (D_j , Å)	normalized pull-off force F_{po}/R (mN/m)	adhesion energy (mJ/m ²)
4	2	179 ± 5	0.05 ± 0.02	0.010 ± 0.004
	30	140 ± 4	0.25 ± 0.06	0.05 ± 0.01
	60	142 ± 4	0.33 ± 0.13	0.07 ± 0.03
9	2	142 ± 4	0.25 ± 0.04	0.054 ± 0.008
	30	132 ± 4	0.59 ± 0.17	0.13 ± 0.04
	60	120 ± 4	0.72 ± 0.24	0.15 ± 0.05
15	2	118 ± 4	0.50 ± 0.10	0.11 ± 0.02
	30	96 ± 4	0.85 ± 0.22	0.18 ± 0.05
	60	93 ± 4	0.95 ± 0.28	0.20 ± 0.06

chains extending over much larger distances. Despite the fact that the salt concentration was negligible, and hence the screening was insignificant, both the magnitude and the range of the repulsive force were much smaller than those measured at pH 8.0. At pH 5.0, the onset of the repulsive force between brushes at 387 Å²/chain occurred at ~ 200 Å. In contrast, at pH 8.0 and 0.01 M NaNO₃, the repulsive force extended to 600 Å. At the higher grafting density, even in 0.1 M NaNO₃ at pH 8 the repulsion extended to > 1000 Å, which is much longer ranged than that at pH 5 in the absence of any screening. Thus, reducing the polymer charge substantially decreased L and, hence, the range and magnitude of the intersurface repulsion.

Another significant change was the onset of adhesion between the polymer layers. This was evident from the noticeable hysteresis between the advancing (loading) and receding (unloading) curves (Figure 5B). During separation of the brushes, the force decreased with separation to about 90 Å, and then the surfaces slowly jumped out of adhesive contact from 100 ± 10 Å (Figure 5B). The force at which adhesive failure occurred is the pull-off force, F_{po} . According to the Johnson–Kendall–Roberts theory of the adhesion between deformable solids, F_{po} is related to the adhesion energy per area between the brushes by $E = F_{po}/1.5\pi R$.^{23,28}

The jump off positions—that is, the distances at which we detected adhesive failure—depended on the time in contact and on the compressive load. The distances from which the two surfaces began to jump out of adhesive contact decreased with increasing compressive load and time in contact (Table 3). This behavior was reproducible and was observed at several different regions of the 2 cm² sample. The observed jumps apart were also very slow at the beginning. The pull off began slowly, and the surfaces finally snapped out of contact at a larger separation. The dynamics of the pull-off depended on the applied force and time in contact. Under conditions where the adhesion was weak, if the measurements were not performed sufficiently slowly, the jump-out was easily missed. However, under conditions that generated stronger adhesion, i.e., greater number of interchain bonds, adhesive failure occurred abruptly.

At pH 5, the magnitude of the adhesion also increased with the grafting density. Similar measurements were carried out between the copolymer brushes at a grafting density of 387 Å²/chain. As expected, the chain extension, and hence the range of the repulsion, increased with grafting density. The compressed polymer thickness similarly increased. However, as shown in Table 3, despite

(28) Efremova, N. V.; Sheth, S. R.; Leckband, D. E. *Langmuir* **2001**, *17*, 7628–7636.

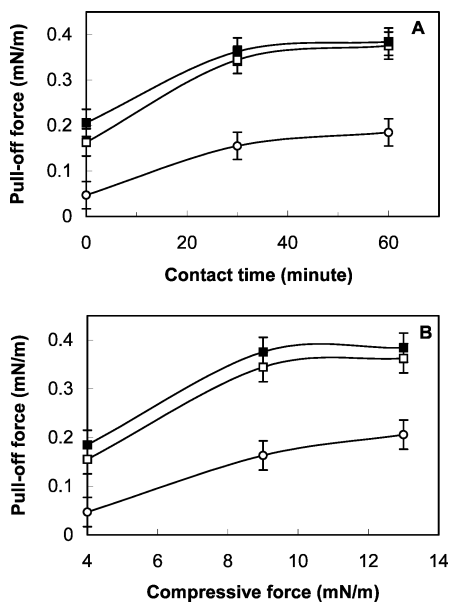


Figure 6. The pull-off force between 4 mol % NIPAM-N-Gly-(C₁₈)₂ monolayers at pH 5. Measurements were carried out at 25 °C in pure water in the absence of added NaNO₃. (A) Change in adhesion with contact time. The open circles correspond to a compressive load of 4 mN/m, the open squares to 9 mN/m, and the filled squares to 13 mN/m. (B) Change in adhesion with the compressive force. The open circles correspond to a contact time of 2 min, the open squares to 30 min, and the filled squares to 60 min.

the increased repulsion, the adhesion between the denser polymer layers is greater. This is as expected since a higher density of polymers per unit volume allows for the formation of a larger number of H bonds, and hence greater adhesion.

To quantify the impact of the ionic strength on the NIPAM-N-Gly-(C₁₈)₂ polymer at pH 5.0, the same experiment was carried out in 0.1 M NaNO₃ and at a polymer grafting density of 1048 Å²/chain (Figure 4A). Changing the salt concentration had little impact on the range and magnitude of the long-ranged force. The magnitude of the force is only slightly smaller than that in the absence of salt, indicating that there is much less charge along the polymer backbone. Thus, the polymer extension *L* and the long-ranged force are fairly insensitive to the ionic strength. However, in 0.1 M NaNO₃ the adhesion was completely extinguished.

Polymer Relaxation and Time-Dependent Behavior. The magnitude of the adhesion at pH 5 depends both on the magnitude of the compressive force and on the time that surfaces were kept in contact. We studied the changes in intersurface adhesion as a function of the compressive force and the time in contact at grafting densities of 1048 Å²/chain (4 mol %; Figure 6) and 387 Å²/chain (10 mol %; Figure 7). At a grafting density of 1048 Å²/chain, the compressive forces used were 4, 9, and 13 mN/m, and the contact times were 2, 30, and 60 min at each load (Figure 6). In the latter case, the magnitude of the pull-off force increased with contact time and then leveled out around 9 mN/m. At 387 Å²/chain, we used compressive forces of 15, 39, and 77 mN/m and contact times of 2, 30, and 60 min, respectively (Figure 7). In this case, the pull-off force continued to increase with the applied pressure, even up to compressive loads of 77 mN/m. At similar 60-min incubation times, the adhesion did not reach a limiting value.

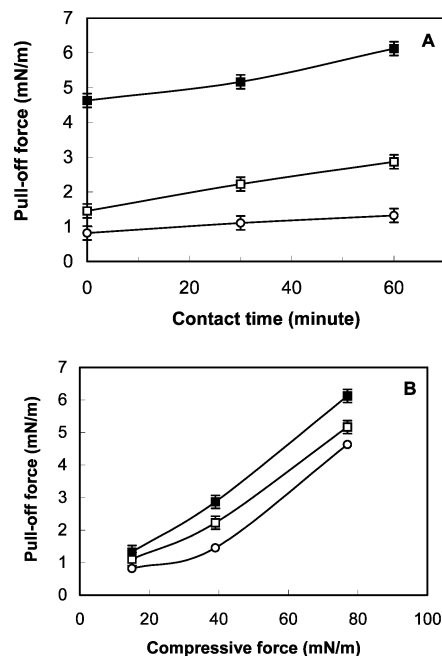


Figure 7. The pull-off force between 10 mol % NIPAM-N-Gly-(C₁₈)₂ monolayers at pH 5. Measurements were carried out at 25 °C in water in the absence of added NaNO₃. (A) The change in adhesion with contact time. The open circles correspond to a compressive load of 15 mN/m, the open squares to 39 mN/m, and the filled squares to 77 mN/m. (B) The change in adhesion with compressive force. The open circles correspond to 2 min, the open squares to 30 min, and the filled squares to 60 min.

Discussion

These studies reveal the molecular basis of the substantial, pH-dependent changes in the interfacial properties of grafted NIPAM-N-Gly-(C₁₈)₂ films. At high pH, the polymer behavior exhibits features characteristic of a polyelectrolyte brush, but a drop in pH switches the polymer film from self-repelling to self-attracting. The brushes collapse and adhere to each other. This differs from polymer collapse due to temperature-dependent changes in solvent quality, since the chains in these experiments are in good solvent. These studies were all carried out at 25 °C, which is well below the LCST of >54 °C for this copolymer. Nevertheless, these direct measurements reveal the qualitative and quantitative changes in the molecular properties of these polymer brushes under different solution conditions. They further reveal the molecular origins of pH-dependent solubility changes of liposomes coated with this material.²¹

These findings thus delineate design rules for tuning the properties of NIPAM-N-Gly-(C₁₈)₂ brushes. At high pH, the polymer interactions are relatively well described by scaling theory for polyelectrolyte brushes, exhibiting universal scaling behavior when appropriately scaled by *C_s* and by *f*². Thus, the thickness and interactions can be tuned according to eqs 3 and 4.

The high pH behavior does differ from that of ideal chains in good solvent. First, although the exponents describing the power law decay are close to unity, they exceed the predicted value of unity in all cases. Additionally, the long-ranged decay lengths exceed the Debye lengths, which are 14, 10, and 3.0 Å, respectively, for 0.01, 0.1, and 1 M NaNO₃ solutions. These deviations could be due to the high polydispersity, *M_n*/*M_w* = 1.7, of the polymer we used. However, similar deviations at large distances were reported with a different polyelectrolyte with a

polydispersity of 1.1.²⁹ The large decay length suggests that some chains may be more extended than those predicted for polyelectrolytes in good solvent. Masra and Tirrell predicted that the segment density profiles of polyelectrolytes in increasingly poor solvents could adopt a denser phase near the surface with more dilute, extended chains at the outer periphery.³⁰ Such dilute outer chains could account for these anomalous long-ranged forces. This could be verified by X-ray reflectivity measurements of the segment density profiles of the grafted chains.³¹

There are two reasons for the decrease in the long-range decay length with increasing salt concentration: namely, the polyelectrolyte extension L decreases with the salt concentration, and salt screens the electrostatic double layer force at $D > L$. The brush extension L is predicted to scale with the salt concentration according to $L \sim C_s^{-1/3}$.²⁷ Between neutral polymers, the extension L that was determined from the range of the osmotic force between polymer brushes agreed with theory and with X-ray reflectivity measurements.^{31,32} Here, however, we could not determine L from force data alone because the repulsive force is a superposition of the electrostatic double layer repulsion and the osmotic force between the chains. Moreover, both depend on the ionic strength, making it difficult to deconvolute these contributions from force-distance measurements alone. Nevertheless, the qualitative trends agreed with the predicted behavior. Increasing the salt concentration from 0.1 to 1 M nearly halved the range of the repulsion from 750 to 350 Å.

There are several notable features of the significant changes in the polymer properties at low pH. First, the reduction in monomer repulsion caused the brushes to collapse, and the increased contribution from H-bonding led to interchain and intrachain adhesion. Schneider and co-workers proposed that increasing the pH from 6 to 8 charged the glycines, by deprotonating the exposed, terminal carboxylic acid.^{19,33} At pH 5.0, a considerable number of carboxyl groups will be protonated, and these can in turn hydrogen bond with other glycines as shown in Figure 8. The reduced charge along the polymer backbone would reduce the electrostatic repulsion between chains, allowing greater interpenetration of chains from opposing brushes. Moreover, adhesion develops when the increased attraction due to the putative H-bonding between amide and carboxyl groups (Figure 8) exceeds the electrostatic repulsion.

Second, the polymer interactions are time dependent, and the dynamics depend on the grafting density. The glycine-glycine adhesion develops with time, presumably as the opposed polymers interpenetrate and increase their effective contact area.³⁴ The osmotic and electrostatic penalty for chain interpenetration would increase with

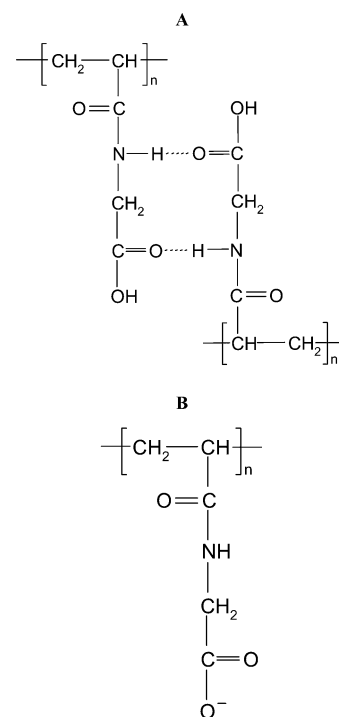


Figure 8. Hypothetical side chain hydrogen bonding as a function of pH. (A) At pH 5.0, the carboxyl groups were protonated and form hydrogen bonds with amide groups. (B) At pH 8.0, the carboxyl groups were deprotonated and negatively charged. The charge generates electrostatic repulsion between surfaces.

increasing grafting density, so that the rate of increase would correspondingly decrease. There is a tradeoff however since the overall adhesion increases with grafting density at the same time that the rate of increase in adhesion decreases. Thus, although robust adhesion would develop more quickly with the more dilute chains, the initial adhesion may still be higher between the denser brushes than the fully developed adhesion between dilute ones.

Conclusions

Using direct force measurements, we have elucidated the molecular basis of experimentally observed, pH-dependent interactions between NIPAM-Gly-(C₁₈)₂-coated liposomes. We further quantified the dependence of the brush properties on a variety of design parameters such as ionic strength and grafting density. These findings will facilitate the rational design of NIPAM-Gly coatings with interfacial properties that are defined at an unprecedented level of detail. These results reveal, for example, the different properties that end-grafted NIPAM-N-Gly-(C₁₈)₂ would exhibit in blood, in lysosomes, or in the stomach. They further define the underlying principles for precisely tuning the interfacial properties in ways that may expand the range of uses of this material.

Acknowledgment. This work was supported by DOE award number DEFGO2-91ER45439.

LA0354382

(29) Abraham, T.; Giasson, S.; Gohy, J. F.; Jerome, R. *Langmuir* **2000**, *16*, 4286–4292.

(30) Misra, S.; Tirrell, M. *Macromolecules* **1996**, *29*, 6056–6060.

(31) Majewski, J.; Kuhl, T. L.; Gerstenberg, M. C.; Israelachvili, J. N.; Smith, G. S. *J. Phys. Chem.* **1997**, *101*, 3122–3129.

(32) Sheth, S.; Efremova, N.; Leckband, D. *J. Phys. Chem B* **2000**, *104*, 7652–7662.

(33) Schneider, J.; Berndt, P.; Haverstick, K.; Kumar, S.; Chiruvolu, S.; Tirrell, M. *Langmuir* **2002**, *18*, 3923–3931.

(34) Leckband, D.; Israelachvili, J. N. *Q. Rev. Biophys.* **2001**, *34*, 105–267.